J Mater Sci (2007) 42:9654–9662
DOI 10.1007/s10853-007-1964-4

Characterization of atmospheric corrosion products of zinc exposed to SO_2 and NO_2 using XPS and GIXD

Juan G. Castaño · Carlos Arroyave · Manuel Morcillo

Received: 10 March 2006 / Accepted: 22 June 2007 / Published online: 31 July 2007

Abstract A complete characterization of corrosion products formed on zinc plates after exposure in a climatic chamber was conducted in this study. The dry deposition of NO_2, SO_2, and $SO_2 + NO_2$, at 25 °C and 35 °C, and relative humidity (RH) of 90% was simulated. Pollutant concentrations evaluated were selected to represent highly polluted industrial atmospheric levels. Analysis techniques included X-ray Photoelectron Spectroscopy (XPS) and Grazing Incidence X-ray Diffraction (GIXD). For tests conducted at 25 °C, the relative amount of sulfate was determined to be higher in the $SO_2 + NO_2$ atmosphere than in the SO_2 atmosphere, and was associated with greater corrosivity in the former atmosphere. NO_2 had an indirect role as a catalyst for SO_2 reduction to sulfate, as evidenced by the greater proportion of sulfate ions detected and the lack of nitrogen compounds in corrosion products. At 35 °C, effect of NO_2 was reduced, and was complicated by a greater tendency for drying so that it was more difficult to maintain the humidity layer. Therefore, no accelerating effect of exposure temperature was observed.

Introduction

Extensive research has been conducted on the atmospheric corrosion resistance of different types of zinc coatings, given their broad application in diverse sectors, like coating for corrosion protection of steel [1–6]. The automotive industry is an important market for zinc-coated steels, although these are also widely used in the construction industry and in manufacturing electronic equipment.

The crucial SO_2 effect in zinc atmospheric corrosion has been corroborated through a large number of studies [7–9]. When the critical relative humidity is reached, the SO_2 adsorbed in the humidity layer that forms on zinc is transformed into sulfite and, subsequently, into sulfate. The humidity layer is acidified by the oxidation of the SO_2 to sulfate, which greatly accelerates the rate of corrosion.

In the past decade, Odnevall and Leygraf [10] made a 90-day, systematic study of atmospheric corrosion of zinc exposed to different atmospheres. They proposed a sequence of formation of corrosion products for the various atmospheres. In most cases, all main corrosion products can be detected after one month of atmospheric exposure. In aggressive atmospheres (marine and industrial) the formation of sulfur and chlorine compounds is very fast (often in a single day). While the process advances, these compounds generally increase in amount, although some can disappear as a result of their transformation into other components, depending on the atmosphere.

For nearly 20 years, some investigators have studied the role of NO_2 in the atmospheric corrosion of metals [11–16]. In particular, it is important to be aware of the NO_2 effect, since its effect in the corrosive phenomenon, although slight, can cause the premature failure of zinc coatings. This can be especially important in situations where zinc is used in electronic equipment components.

J. G. Castaño (✉) · C. Arroyave
Corrosion and Protection Group, Department of Materials
Engineering, Universidad de Antioquia, P.O. Box 1226,
Medellin, Colombia
e-mail: jcasta@udea.edu.co

M. Morcillo
National Center for Metallurgical Research – CENIM, Avda.
Gregorio del Amo 8, 28040 Madrid, Spain

General consensus exists concerning the negligible effect of NO_2 when it acts alone in laboratory tests. In contrast, for NO_2 acting together with sulfur dioxide, there is no consensus. Some researchers report an accelerant effect of both polluting agents upon zinc [12, 13], due to the increase in the speed of sulfite oxidation to sulfate in the presence of NO_2, where the latter participates indirectly in the corrosion process, like a catalyst. Other authors affirm that NO_2 participates directly in the chemical reactions of the process of corrosion, as in products already formed [14]. On the other hand, some researchers were unable to find any synergistic effect between SO_2 and NO_2 [15, 16].

In this work, the role of NO_2 in the atmospheric corrosion of zinc was analyzed from a detailed characterization of corrosion products. Laboratory tests with exposure parameters close to the conditions observed in real atmospheres were performed, with the aim of simulating close-to-reality corrosion mechanisms. Low-pollutant concentrations and short-term exposures were carried out. For these reasons, characterization techniques applicable for the analysis of very thin corrosion layers were used: X-ray Photoelectron Spectroscopy (XPS) and Grazing Incidence X-ray Diffraction (GIXD).

Experimental

Exposure was conducted in a HERAEUS HC2033 climatic chamber with gaseous pollutant dosage system, laminar air flow of 1 $m^3 h^{-1}$, plus a rate of pollutants (SO_2 and/or NO_2) mixed with N_2 from a gas pipe, and the desired levels of RH and temperature strictly controlled. Commercial grade zinc plates, $100 \times 50 \times 0.6$ mm^3 in size, were used. Surface preparation of the zinc plates consisted of dry sandpapering with silicon carbide abrasive papers (abrasion numbers 240, 320, 400, and 600), degreasing with acetone of absolute degree and detergent, cleaning by means of ultrasonic agitation with ethanol during 15 min and drying in a hot air jet. Experiments were performed using the gas concentrations given in Table 1.

The concentration value of polluting agents (800 $\mu g\ m^{-3}$) examined corresponds to concentration levels detected during periods of very high contamination in industrial atmospheres. For all experiments, the relative humidity (RH) was 90 ± 5%. Tests were conducted at 25 ± 1 °C and 35 ± 1 °C, with exposure times of 7 and 14 days.

Table 1 Pollutant levels for simulated atmospheres in a climatic chamber

Atmosphere	SO_2 concentration ($\mu g\ m^{-3}$)	NO_2 concentration ($\mu g\ m^{-3}$)
Without pollutants	0	0
SO_2	800	0
NO_2	0	800
$SO_2 + NO_2$	800	800

The corrosion products were characterized by GIXD using a SIEMENS D5000 diffractometer with Cu anode radiation (Cu_{ka}, $\lambda = 1.5406$ Å), operating at 40 kV and 40 mA. The incidence angle was 0.7° and scanning speed was 1 s, from $2\theta = 4°$ to $2\theta = 90°$.

Photoelectron spectra were recorded by using a Fisons MT500 spectrometer equipped with a hemispherical electron analyzer (CLAM 2) and an MgKα X-ray source operated at 300 W. The samples were mechanically fixed onto small flat discs supported by an XYZ manipulator placed in the analysis chamber. The residual pressure in this ion-pumped analysis chamber was maintained below 5×10^{-7} Pa during data acquisition. Spectra were collected for 20–90 min, depending on peak intensities at pass energies of 10 eV (for high resolution spectra) and 50 eV (for the general spectra). High-resolution spectra were recorded for C1s, O1s, N1s, Zn2p, ZnLMM (Auger) and S2p. The intensities were estimated by calculating the area under each peak after smoothing and subtraction of the S-shaped background using the Shirley's method and fitting the experimental curve to a mix of Lorentzian and Gaussian lines of variable proportions. Although sample charging was observed, accurate binding energies (BE) could be determined by referencing to the adventitious C1s peak at 284.8 eV. The compositions were evaluated from peak intensity ratios and reported atomic sensitivity factors [17].

Results

Grazing incidence X-ray diffraction (GIXD)

After 14 days of climatic chamber exposure, similar results were obtained at 35 °C and 25 °C. In atmospheres without pollutants and atmospheres with NO_2, only metallic zinc was detected. In SO_2 and $SO_2 + NO_2$ atmospheres, trihydrated zinc hydroxysulfate, $Zn_4SO_4(OH)_6{\cdot}3H_2O$, was found. Figures 1 and 2 show GIXD general spectra of zinc exposed to SO_2 and $SO_2 + NO_2$ atmospheres. The hydroxysulfate main peak at $2\theta = 9.4$ indicates a *d*-spacing between planes of 9.398 Å ((002) planes and maximum relative intensity equal to 100). A second hydroxysulfate peak appears at $2\theta = 18.9$, corresponding to a *d*-spacing of 4.702 Å ((004) planes and maximum relative intensity equal to 95), according to JCPDS cards [18]. At 25 °C, the presence of zinc hydroxysulfate in $SO_2 + NO_2$ atmospheres was more prominent.

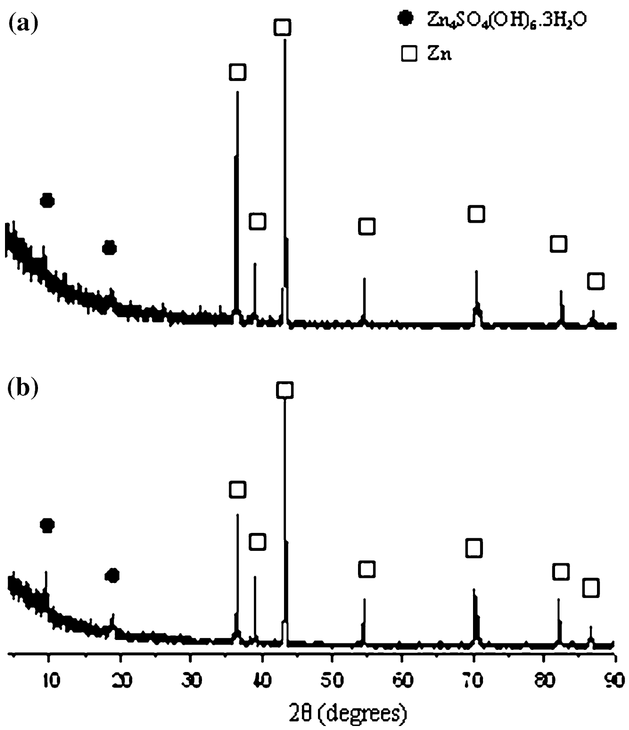

Fig. 1 Results of GIXD studies performed on zinc exposed for 14 days at 35 °C: (**a**) SO_2 and (**b**) $SO_2 + NO_2$ atmospheres

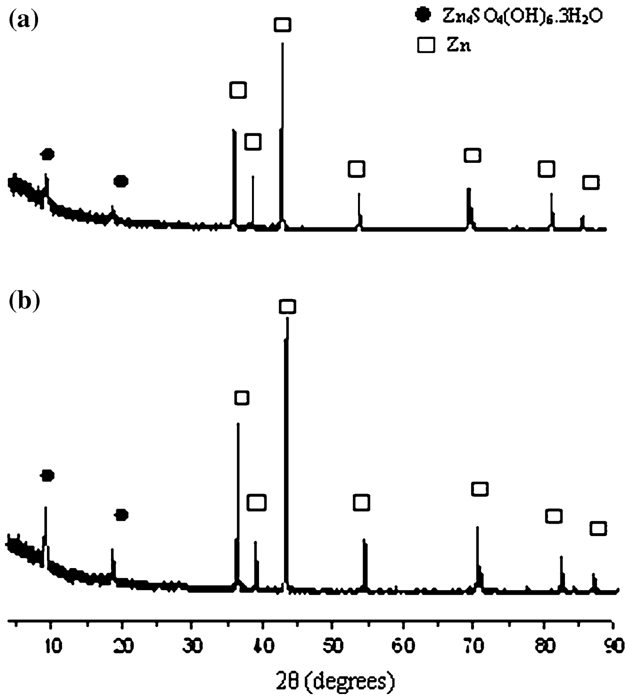

Fig. 2 Results of GIXD studies performed on zinc exposed for 14 days at 25 °C: (**a**) SO_2 and (**b**) $SO_2 + NO_2$ atmospheres

X-ray photoelectron spectroscopy (XPS)

To obtain reference spectra and corroborate the quality of surface cleaning prior to the tests, a zinc plate was cleaned and analyzed by XPS without chamber exposure. High-resolution XPS spectra and Auger spectra of a non-sputtered zinc surface and after 1 min sputtering with argon were obtained. Figure 3 shows carbon (C1s), oxygen (O1s), zinc (Zn2p), and zinc (Auger) spectra. In the C1s spectra, the most intense component situated at 284.8 eV may be attributed to the presence of C–C/C–H groups. At room temperature, the metal surface in contact with the atmosphere becomes instantaneously coated with a thin film of C–C/C–H groups. Another component situated at 288.8 is associated to the presence of carboxyl-type groups (O = C–O), which may indicate the presence of residues of oils used to protect the metal surface during storage and not completely removed by the ultrasound cleaning treatment. After sputtering for 1 min, the intensities of the two main components of C1s peak were substantially reduced.

In the O1s spectra, two components may be differentiated: the component at 531.8 eV is associated to the OH^- ion and the component at 530.5 eV may be associated to the presence of oxygen in the form of zinc oxide (ZnO). Before sputtering, the most intense peak corresponds to the first component, whereas after sputtering, the hydroxyl component is reduced and the ZnO component increases, indicating that a thin ZnO layer is formed adjacent to the metal surface. The zinc spectra shows a single component at 1021.8 eV that includes metallic zinc and zinc oxide. Since the resolution of the spectrometer used in this study is greater than the difference in the energies of Zn in metallic and oxidized states, it was not possible to determine the proportion of zinc in each state, although the peak intensity increases with sputtering. In the ZnLMM Auger spectra, the difference between the kinetic energies of the components associated to Zn in metallic and oxidized states is more than 4 eV. Each spectrum contains two components that may be associated to the presence of metallic Zn (261.1 eV) and oxidized zinc (265.9 eV). Both increase with sputtering.

Figures 4 and 5 show high-resolution O1s, N1s, and S2p XPS spectra acquired on the surface of zinc exposed at 35 °C during 7 and 14 days. C1s spectra are not included because species related to zinc corrosion products were not found in these.

The spectra acquired from the zinc specimen exposed at 35 °C for 7 days in SO_2 (S) and $SO_2 + NO_2$ (S + N) atmospheres are presented in Fig. 4. In both atmospheres, the high O1s spectrum has a main component at 531.8 eV, which includes the contribution of SO_3^{2-}, SO_4^{2-} and OH^- ions. The high-resolution N1s spectrum does not reveal the presence of any nitrogen compound. Two components are

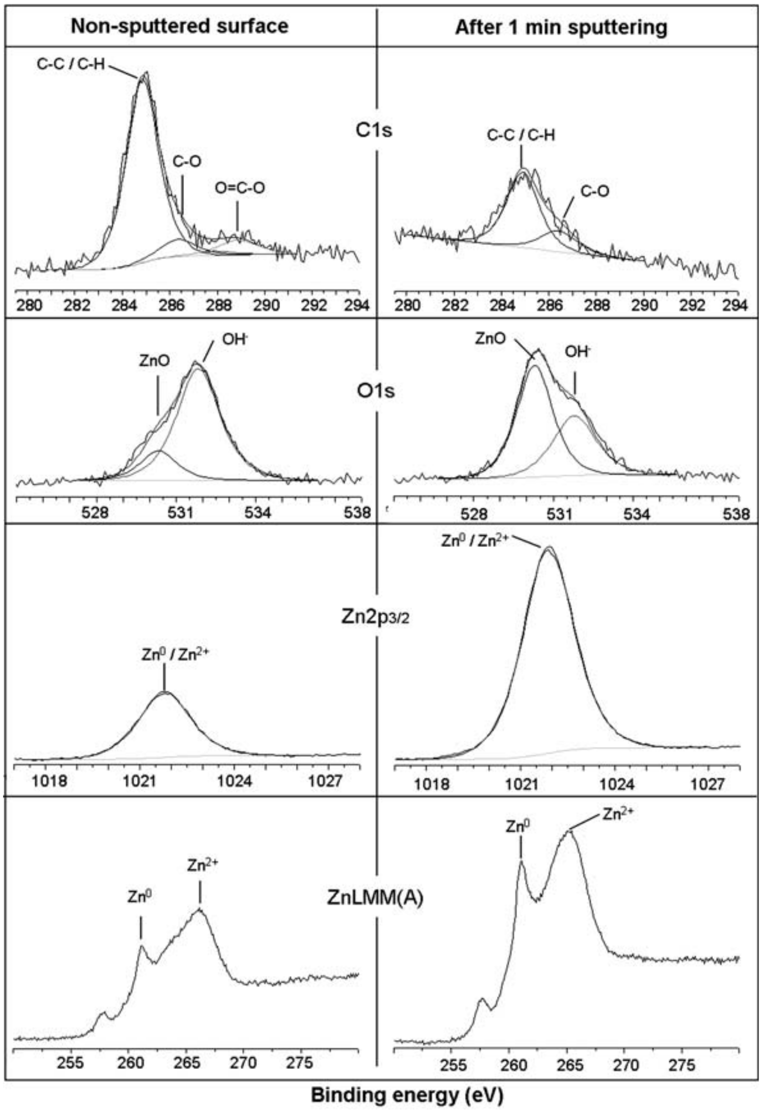

Fig. 3 Evolution of high-resolution C1s, O1s, Zn2p XPS spectra and ZnLMM Auger spectra acquired on the surface of unexposed zinc

differentiated in high-resolution S2p spectra: sulfite ion (167.4 eV), the main component, and sulfate ion (169.4).

Spectra acquired on the zinc specimen after the 14-day exposure at 35 °C in atmospheres without pollutants and in the NO_2 (N), SO_2 (S), and $SO_2 + NO_2$ (S + N) atmospheres are shown in Fig. 5. The components of each peak are similar to those illustrated in Fig. 4.

Figures 6 and 7 show the relative amount of compounds detected in the corrosion products of zinc exposed at 35 °C for periods of 7 and 14 days.

After the 7-day exposure in the NO_2 atmosphere (Fig. 6), the main compounds were zinc hydroxide and zinc oxide. In contrast, after the 7-day exposure in the SO_2 and $SO_2 + NO_2$ atmospheres the main compounds detected were zinc hydroxysulfate and zinc sulfite, with insignificant variations in their relative amounts with respect to the type of atmosphere. After 14 days of exposure in the NO_2 atmosphere (Fig. 7), hydroxide was the main compound present. Zinc oxide was not detected. After comparable exposure in the SO_2 and $SO_2 + NO_2$ atmospheres, the main compounds detected were again zinc hydroxysulfate and zinc sulfite, although the hydroxysulfate amount was somewhat greater in the presence of NO_2.

High-resolution O1s, N1s, and S2p XPS spectra acquired on the surface of the zinc specimen exposed for 7 and 14 days at 25 °C are shown in Figs. 8 and 9. In addition, the relative amount of the compounds identified in corrosion products after 7 and 14 days of exposure at 25 °C are presented in Figs. 10 and 11.

Spectra obtained from the specimen exposed for 7 days in SO_2 (S) and $SO_2 + NO_2$ (S + N) atmospheres at 25 °C are shown in Fig. 8. In both atmospheres, the high O1s spectrum has a main component at 531.8 eV, which includes the contribution of SO_3^{2-}, SO_4^{2-}, and OH^- ions. The

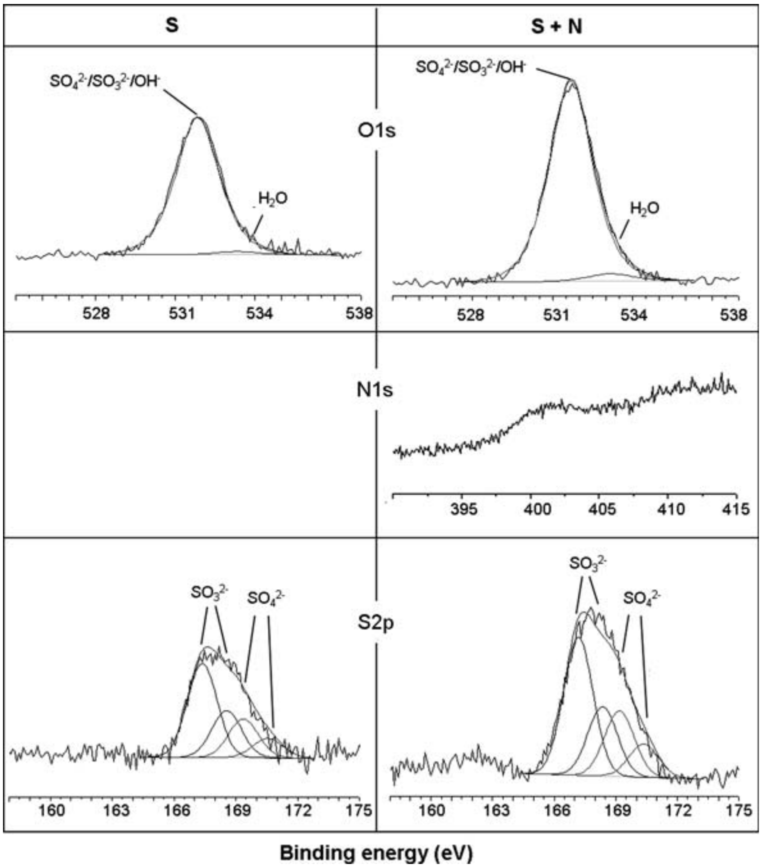

Fig. 4 High-resolution O1s, N1s, and S2p XPS spectra of zinc exposed for 7 days at 35 °C to SO_2 (S) and $SO_2 + NO_2$ (S + N) atmospheres

high-resolution N1s spectrum does not demonstrate the presence of any nitrogen compound. Two components are differentiated in high-resolution S2p spectra: sulfite ion at 167.4 eV, which is the main component, and sulfate ion at 169.4 eV.

The spectra obtained from specimens exposed for 14 days in atmospheres without pollutants, and in NO_2(N), SO_2 (S), and $SO_2 + NO_2$ (S + N) atmospheres at 25 °C are shown in Fig. 9. The components of each spectrum are similar to those shown in Fig. 8, but it is clearly noted that in the presence of NO_2, the proportions of sulfate and sulfite were equal.

In the specimens exposed for 7 days in the SO_2 and $SO_2 + NO_2$ atmospheres (Fig. 10), the main compounds formed were zinc sulfite (in greater proportion) and zinc hydroxysulfate, with a small variation in its relative amount with respect to the type of atmosphere.

After 14 days of exposure in the NO_2 atmosphere (Fig. 11), the main constituent identified on the specimen was the hydroxide, although a significant amount of ZnO was detected. For the specimens exposed in the SO_2 and $SO_2 + NO_2$ atmospheres, the main constituents present were zinc hydroxysulfate and zinc sulfite, with a minor percentage of ZnO. In this case, an important increase in sulfate percentage was observed for the specimens exposed in the NO_2 atmosphere, indicating that its presence plays a positive role in the formation of these compounds.

Discussion

XPS analyses (Fig. 3) indicated that a very thin film of ZnO forms instantaneously by chemical oxidation on the zinc surface in contact with clean air at room temperature. This film does not affect the later electrochemical corrosion process [7]. Once the humidity layer is established, zinc hydroxide is rapidly formed on the ZnO film via an electrochemical mechanism. Generally, it is considered that hydroxides are the initial compounds in zinc atmospheric corrosion studies [7, 19].

For zinc exposed for 14 days in atmospheres without pollutants, the presence of ZnO and $Zn(OH)_2$ was established for both temperatures studied (Figs. 5 and 9). Under these conditions, the corrosion process is still incipient. Since air access into the climatic chamber is limited and, therefore, the CO_2 is insufficient, it is only logical that zinc carbonates do not form.

Some $Zn(OH)_2$ and ZnO were observed after exposure in the NO_2 atmosphere, but the incorporation of nitrogen compounds to corrosion products was not verified by the

Fig. 5 High-resolution O1s, N1s, and S2p XPS spectra of zinc exposed for 14 days at 35 °C to atmospheres without pollutants, NO_2 (N), SO_2 (S), and $SO_2 + NO_2$ (S + N) atmospheres

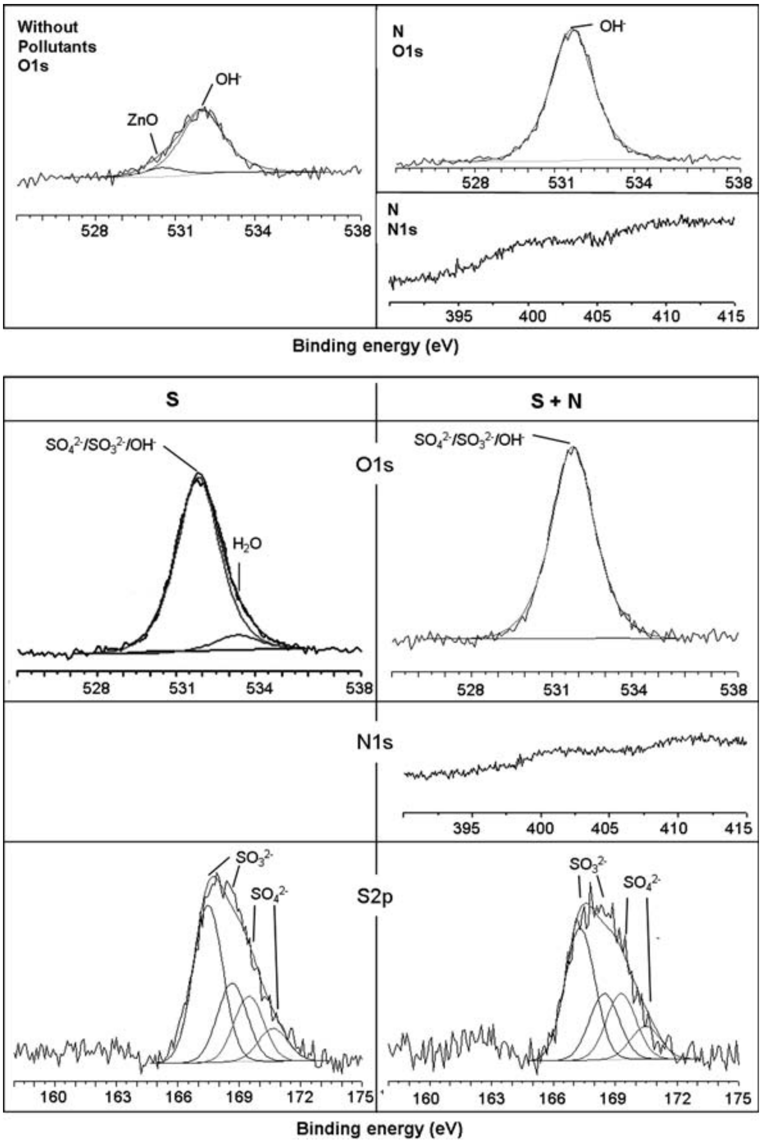

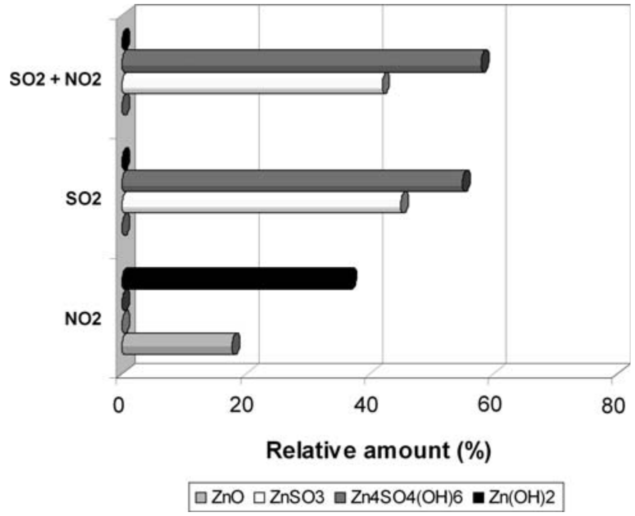

Fig. 6 Relative amount of zinc corrosion products detected after a 7-day exposure at 35 °C under different atmospheres

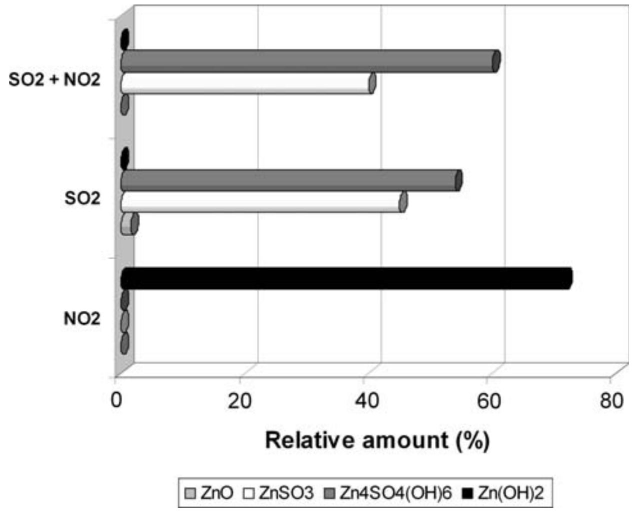

Fig. 7 Relative amount of zinc corrosion products detected after a 14-day exposure at 35 °C under different atmospheres

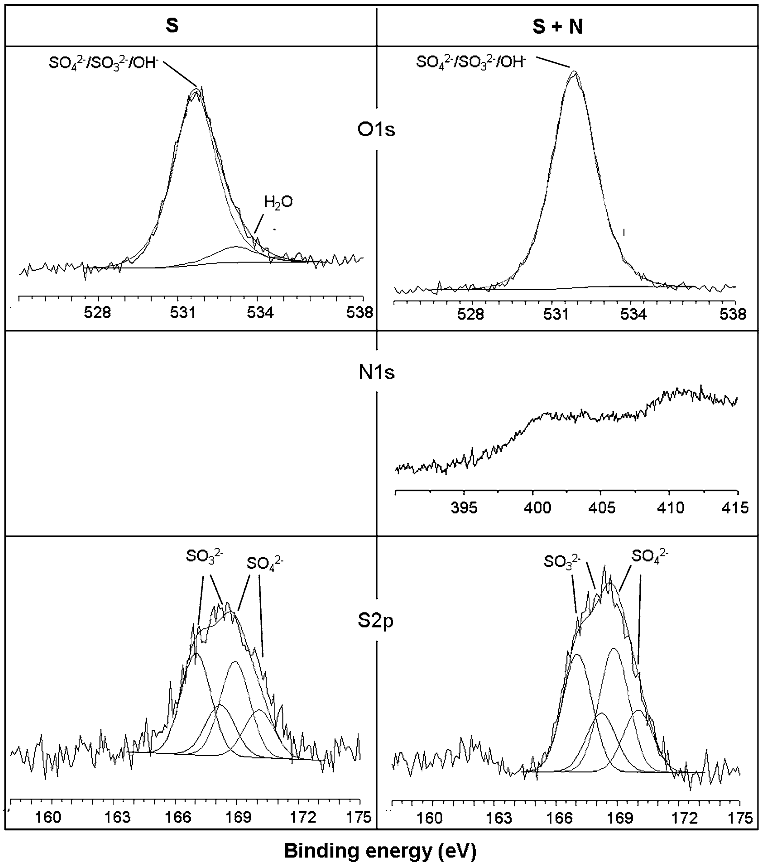

Fig. 8 High-resolution O1s, N1s, and S2p XPS spectra of zinc exposed for 7 days at 25 °C to SO_2 (S) and $SO_2 + NO_2$ (S + N) atmospheres

XPS and GIXD analyses. The corrosion of zinc exposed to this pollutant is very low and after 14 days of exposure only a very thin layer of corrosion products was detected.

In SO_2 atmospheres, there were no significant variations between the corrosion products formed at 35 °C and 25 °C. After the 7-day exposure at 35 °C, XPS analyses (Figs. 4 and 6) revealed that the main constituents were zinc hydroxysulfate and zinc sulfite. After 14 days, the presence of the hydroxysulfate was confirmed by GIXD. After the 7-day exposure at 25 °C, the main constituent was sulfite, whereas after the 14 day exposure the relative amount of hydroxysulfate increased, the relative amount of sulfite decreased, and some oxide appeared.

The reactions for the adsorption process of SO_2 and sulfite and sulfate ion formation are as follows [13]:

$$SO_{2\,(g)} \leftrightarrow SO_{2\,(ads)} \qquad (1)$$

$$SO_{2\,(ads)} + H_2O \leftrightarrow HSO_{3\,(ads)}^{2-} + H^{+}_{(ads)} \qquad (2)$$

$$HSO_{3\,(ads)}^{2-} \leftrightarrow SO_{3\,(ads)}^{2-} + H^{+}_{(ads)} \qquad (3)$$

$$SO_{3\,(ads)}^{2-} + {}^{1}\!/_{2}O_2 \leftrightarrow SO_{4\,(ads)}^{2-} \qquad (4)$$

$$HSO_{3\,(ads)}^{2-} + {}^{1}\!/_{2}O_2 \leftrightarrow SO_{4\,(ads)}^{2-} + H^{+}_{(ads)} \qquad (5)$$

In atmospheres wherein sulfur dioxide acts together with nitrogen dioxide, it is clearly observed by GIXD and XPS analyses of the specimens exposed for 14 days at 25 °C that the hydroxysulfate formation is accelerated. At 35 °C, this effect is not as clear due to the two-fold effect that temperature can have. Just as temperature can have a positive effect upon the kinetics of the chemical reactions and in the diffusion of the agents involved in the corrosive phenomenon, it can also have a negative effect when producing a faster drying of the humidity layer and therefore reducing the necessary "wet" time so corrosion occurs.

Based upon the characterization of the exposed zinc specimens, it has been possible to show an accelerating effect of NO_2, and also that NO_2 was not involved in the corrosion product formation, since the presence of nitrogen was not detected in the analyzed compounds. The increase in the proportion of sulfate ions in atmospheres where the NO_2 accelerating effect was verified suggests that its occurrence is related to the increase in the SO_2 to sulfate oxidation rates due to a catalytic effect. There may be no direct reaction between NO_2 and SO_2.

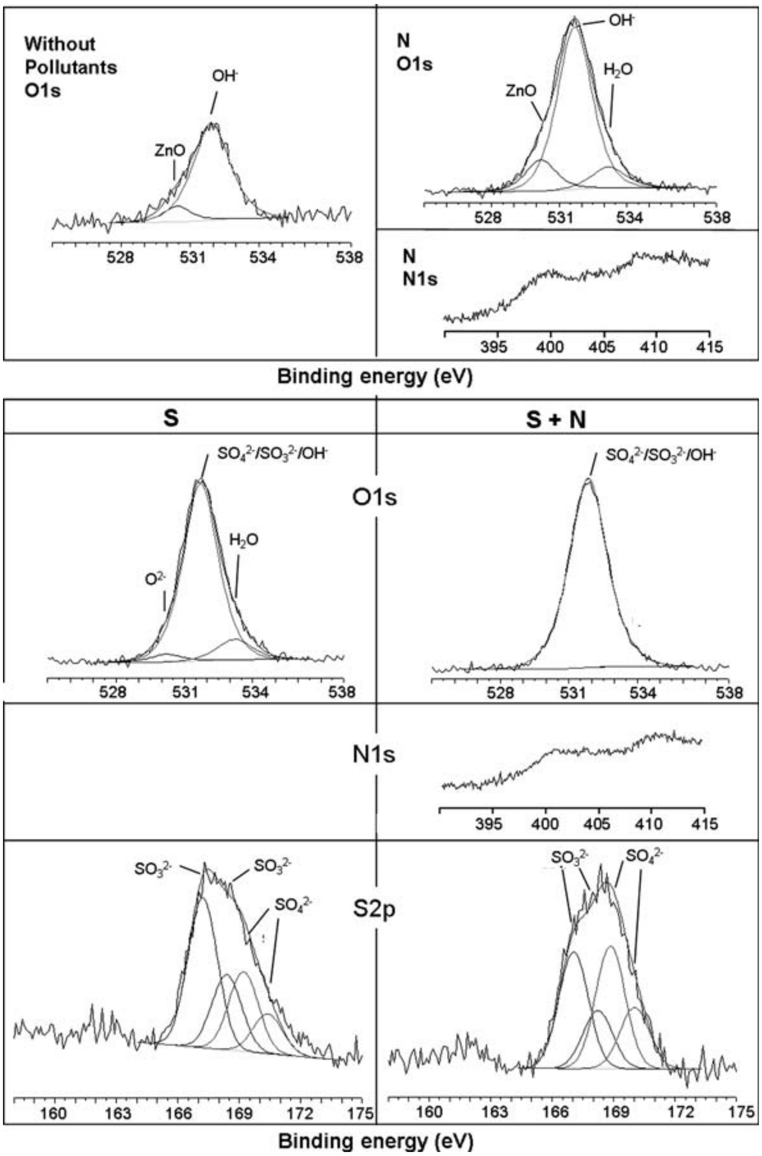

Fig. 9 High-resolution O1s, N1s, and S2p XPS spectra of zinc exposed for 14 days at 25 °C to atmospheres without pollutants, NO_2 (N), SO_2 (S), and SO_2 + NO_2 (S + N) atmospheres

The global process of sulfur dioxide oxidation to sulfate and the catalytic action of nitrogen dioxide proposed in this work would correspond to the following general reactions:

$$SO_2 + H_2O \rightarrow SO_3^{2-} + 2H^+ \quad (6)$$

$$SO_3^{2-} + NO_2 \rightarrow SO_4^{2-} + NO \quad (7)$$

$$NO + {}^1\!/_2O_2 \rightarrow NO_2 \quad (8)$$

$$SO_2 + {}^1\!/_2O_2 + H_2O \rightarrow SO_4^{2-} + 2H^+ \quad (9)$$

where nitrogen dioxide would act as an oxygen carrying agent. The greater oxygen availability would produce an increase in the sulfur dioxide and sulfite oxidation.

Conclusions

In nitrogen dioxide atmospheres, corrosion was minimal, indicating that NO_2 does not promote the corrosion of zinc. $Zn(OH)_2$ and ZnO were detected after exposure in this atmosphere at both 35 °C and 25 °C, with 90% RH. In sulfur atmospheres, zinc corrosion was enhanced, with the formation of a greater amount of corrosion products: mainly zinc hydroxysulfate and sulfite.

In atmospheres with sulfur dioxide and nitrogen dioxide, an accelerant effect was observed at 25 °C and 90% RH, resulting in the formation of a greater proportion of zinc hydroxysulfate. The nitrogen dioxide role was indirect and it acted as a catalyst in the oxidation of sulfur dioxide to sulfate on metal surface. Nitrogen dioxide did not take part

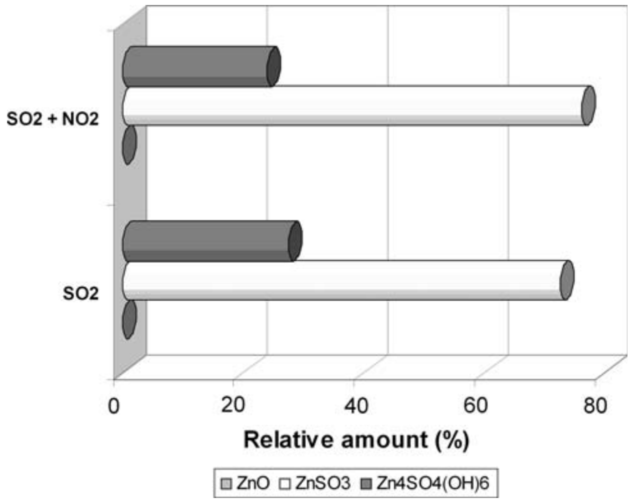

Fig. 10 Relative amount of zinc corrosion products detected after a 7-day exposure at 25 °C under different atmospheres

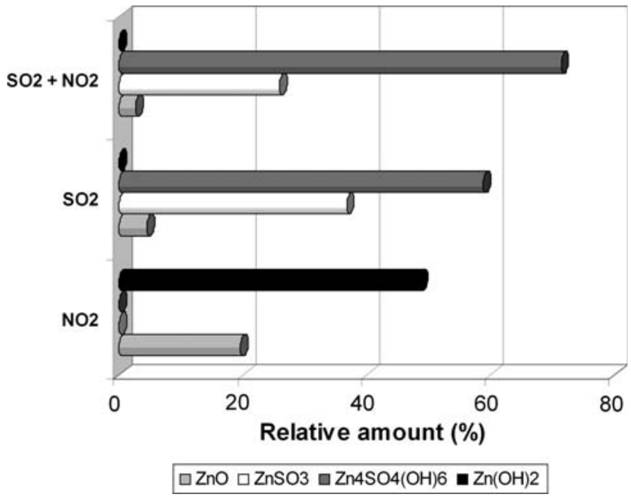

Fig. 11 Relative amount of zinc corrosion products detected after 14-day exposure at 25 °C under different atmospheres

in reactions nor was it present in the corrosion products, consistent with the GIXD and XPS analyses. Temperature had an important effect. It was noted that the samples tested at higher temperature (35 °C) exhibited a greater tendency for drying so that it was more difficult to maintain the humidity layer. Therefore, no accelerating effect of exposure temperature was observed.

Acknowledgements Juan G. Castaño expresses his gratitude to the Corrosion and Protection Group (*Universidad de Antioquia*, Colombia) and the “Francisco José de Caldas” Colombian Institute for the Development of Science and Technology – COLCIENCIAS, for the doctoral grant awarded.

References

1. Panossian Z, Mariaca L, Morcillo M, Flores S, Rocha J, Peña J, Herrera F, Corvo F, Sanchez M, Rincón OT, Pridybailo G, Simancas J (2005) Surf Coat Technol 190:244
2. Tsuru T (2005) In: Proceedings of 16th international corrosion congress, Beijing, China, September 2005
3. Odnevall I (1996) In: Proceedings of 13th international corrosion congress, Melbourne, November 1996, paper 018
4. Muster TH, Cole IS (2004) Corros Sci 46:2319
5. Bhattacharjee AK, Singh I (1995) J Mater Sci 30:1617
6. Feliu S Jr, Barranco V (2003) Acta Mater 51:5413
7. Zhang XG (1996) Corrosion and electrochemistry of zinc. Plenum Press, New York
8. Feliu S, Morcillo M (1978) Rev Metal (Madrid) 14:198
9. Graedel TE (1989) J Electrochem Soc 136:193C
10. Odnevall I, Leygraf C (1995) In: Kirk WW, Lawson H (eds) Atmospheric corrosion, STP 1239. ASTM, Philadelphia, p 215
11. Arroyave C, Morcillo M (1995) Corros Sci 37:293
12. Svensson J-E, Johansson L-G (1993) J Electrochem Soc 140:2210
13. Svensson J-E, Johansson L-G (1993) Corros Sci 34:721
14. Mansfeld F, Jeanjaquet SL, Kending M, Roe DK (1986) Atmos Environ 20:1179
15. Oesch S, Faller M (1997) Corros Sci 39:1505
16. Henriksen JF, Rode A (1986) In: Proceedings of 10th Scandinavian corrosion congress, Stockholm, p 39
17. Briggs D, Seah MP (1990) In: Practical surface analysis, vol 1: Auger and X-ray photoelectron spectroscopy. John Wiley, Chichester, p 635
18. JCPDS-ICDD (1994) Diffraction data cards. Joint Committee on Powder Diffraction Standards, Philadelphia, Card 39–689
19. Morcillo M, Almeida E, Rosales B, Urruchurtu J, Marrocos M (1998) Corrosión y Protección de Metales en las Atmósferas de Iberoamérica, Parte I: Mapas de Iberoamérica de Corrosividad Atmosférica. CYTED, Madrid, p 22